UJEAS

UNIZIK JOURNAL OF ENGINEERING AND APPLIED SCIENCES

UNIZIK Journal of Engineering and Applied Sciences 6(3), September (2026), 3678-3690
Journal homepage: https://journals.unizik.edu.ng/index.php/ujeas
PRINT ISSN: 2992-4383 || ONLINE ISSN: 2992-4391

Low-Carbon Reinforced Concrete Beams Using Recycled-Aggregate Concrete and Industrial-Waste Binders: Experimental Bond-Strength and Flexural Performance Assessment

Unamba K.U.*
Department of Civil Engineering, Taraba State University, Jalingo, Nigeria
Medjor E.A.
Department of Civil Engineering, Taraba State University, Jalingo, Nigeria

Corresponding Author's E-mail: udokanma@tsuniversity.edu.ng

Abstract
The construction sector is one of the largest contributors to global carbon dioxide emissions, with Portland cement production accounting for roughly 8% of anthropogenic CO2 annually. This paper presents an experimental investigation into the bond strength and flexural performance of reinforced concrete beams made from recycled coarse aggregate concrete incorporating industrial-waste supplementary cementitious materials, specifically ground granulated blast-furnace slag conforming to EN 15167-1, fly ash conforming to EN 450-1, and silica fume conforming to EN 13263-1. Four concrete mixes were evaluated: a normal concrete control, two recycled aggregate concrete mixes with 50% and 100% coarse aggregate replacement, and a blended-binder mix with 100% recycled aggregate and combined supplementary cementitious material substitution of 44.4% by cement mass. Beams measuring 150 mm x 250 mm x 2000 mm were tested under four-point bending at 28 days, with companion cylinder and pull-out specimens tested in parallel. The characteristic compressive strength of the 100% recycled aggregate mix fell 15.8% below the normal concrete control (34.7 vs. 41.2 MPa), while the blended-binder mix surpassed normal concrete by 5.6% at 43.5 MPa. Experimental bond strength in the blended-binder mix reached 10.53 MPa, exceeding normal concrete by 7.0%, while the 100% recycled aggregate mix showed a 16.6% reduction. Eurocode 2 design bond values proved conservative relative to measured results across all mixes, with the fib Model Code 2010 showing markedly closer agreement. The blended-binder mix achieved an ultimate load of 134.7 kN and a ductility index of 4.12 against normal concrete's 3.41. Embodied carbon analysis confirmed a 28.3% reduction for the blended-binder mix relative to the normal concrete control.
Keywords: Recycled aggregate concrete; supplementary cementitious materials; Eurocode 2; bond strength; flexural performance; interfacial transition zone; embodied carbon

1. Introduction

Concrete is the most widely consumed manufactured material on earth, with Portland cement production exceeding 4.1 billion tonnes in 2022 and releasing approximately 2.9 billion tonnes of CO2 in the process (IEA/WBCSD 2021). Urbanisation across sub-Saharan Africa, South Asia, and Southeast Asia is projected to drive a 40 to 55% increase in concrete demand before 2050 (Habert et al. 2020), making decarbonisation of the cement and concrete sector both a technical and economic priority. At the same time, construction and demolition waste generation has reached 3 to 5 billion tonnes per annum worldwide, with coarse aggregate fragments accounting for up to 75% of this stream by mass (Silva et al. 2019). European legislation, including the Waste Framework Directive 2008/98/EC and its successor provisions under the European Green Deal, increasingly mandates diversion of construction and demolition waste from landfill and valorisation of secondary materials in structural applications. In this context, recycled aggregate concrete incorporating industrial-waste supplementary cementitious materials has attracted sustained research interest. However, the combined influence of high recycled coarse aggregate substitution rates and blended binder systems on reinforcement bond behaviour and beam-level structural performance, evaluated within a Eurocode design framework, remains incompletely characterized.

Portland cement clinker production is intrinsically energy-intensive, requiring kiln temperatures of approximately 1,450 degrees Celsius and generating CO2 through both fuel combustion and the decarbonation of calcium carbonate. EN 197-1 cement types that partially replace clinker with supplementary cementitious materials offer an established route to lower embodied carbon while maintaining structural-grade performance. Ground granulated blast-furnace slag conforming to EN 15167-1 behaves as a latent hydraulic binder, reacting with calcium hydroxide liberated during CEM I hydration to produce additional calcium silicate hydrate gel. Fly ash conforming to EN 450-1 Class S contributes more slowly through pozzolanic reaction, densifying the paste microstructure over weeks to months. Silica fume conforming to EN 13263-1 operates simultaneously as an ultra-fine physical filler and a highly reactive pozzolan, with documented reductions in interfacial transition zone porosity of up to 30% at

substitution levels of 5 to 10% (Lothenbach et al. 2011; Juenger and Siddique 2015; Mehta and Monteiro 2014). When these materials are used together, their reactions tend to complement rather than simply add to each other, because the slag and fly ash reaction products provide additional activation sites and pore-filling mass that extends the densification beyond what each supplementary cementitious material achieves independently.

The interfacial transition zone between hardened cement paste and aggregate is widely regarded as the structurally critical zone in conventional concrete, owing to the localised water-rich region that forms around aggregate particles during mixing and leaves a porous, calcium hydroxide-rich layer after hydration (Scrivener et al. 2004). In recycled aggregate concrete, this issue is amplified by the attached mortar layer adhering to the surface of crushed concrete aggregates, introducing a second, potentially weaker interfacial transition zone alongside the primary one. Research has consistently shown that this double-zone phenomenon raises porosity, increases water absorption, and reduces mechanical stiffness and strength relative to natural aggregate concrete at equivalent mix proportions (Bravo et al. 2015; Tam et al. 2018; Kou et al. 2011). Compressive strength reductions of 12 to 22% have been reported for full recycled coarse aggregate substitution (Zhu et al. 2016), and elastic modulus decreases of 9 to 18% have been documented for 100% replacement (Pedro et al. 2017). Bond strength, which governs reinforcement anchorage and development length under EN 1992-1-1 provisions, is equally sensitive to interfacial integrity, because the bearing resistance of the concrete keys against bar ribs depends directly on the tensile and compressive capacity of the surrounding paste (Zhao et al. 2008).

Several research groups have investigated supplementary cementitious material additions as a means of compensating for recycled aggregate concrete's inherent weaknesses. Kou and Poon (2015) showed that replacing 25 to 50% of CEM I with ground granulated blast-furnace slag in recycled aggregate concrete improved 90-day compressive strength above comparable normal concrete values. Xiao et al. (2012) reported that binary fly ash and CEM I systems reduced interfacial transition zone microcracking in recycled aggregate concrete under sustained loading. What is less well documented is the systematic combination of a triple supplementary cementitious material blend with 100% recycled coarse aggregate in structural beams, tested for both reinforcement bond and four-point flexural response, with results analysed against EN 1992-1-1 and the fib Model Code 2010 (fib 2013) predictions. The specific objectives of the present study are: (i) to characterise the mechanical and bond properties of four recycled aggregate concrete mixes with varying recycled coarse aggregate content and supplementary cementitious material combinations; (ii) to evaluate the load-deflection response, cracking behaviour, and ductility of reinforced concrete beams fabricated from those mixes; (iii) to compare experimental bond-strength data with EN 1992-1-1 and Model Code 2010 code predictions; (iv) to quantify embodied CO2 savings; and (v) to propose a calibrated empirical bond-strength model for deformed bars in recycled aggregate concrete.

2.0 Materials and Methods

2.1 Materials

Cement used throughout was CEM I 52.5N conforming to EN 197-1 (CEN 2000), with a specific gravity of 3.15 and a Blaine fineness of 350 m2/kg. Ground granulated blast-furnace slag conforming to EN 15167-1 (CEN 2012a), with an activity index of 86% at 28 days, was sourced from a local integrated steelmaking facility. Fly ash conforming to EN 450-1 Class S (CEN 2012b), fineness category N, was obtained from a coal-fired power station; its combined reactive oxide content of 79.5% exceeded the standard minimum of 70%. Silica fume conforming to EN 13263-1 (CEN 2009a) was supplied in densified powder form with SiO2 content of 93.2% and a 28-day activity index of 108%, confirming high reactivity. Physicochemical properties of all binders are summarised in Table 1.

Table 1: Physicochemical Properties of Cementitious Materials

Property	CEM I 52.5N	GGBS (EN 15167-1)	Fly Ash (EN 450-1)	Silica Fume (EN 13263-1)
Specific gravity	3.15	2.90	2.30	2.20
Blaine fineness (m2/kg)	350	420	380	18,000
SiO2 + Al2O3 + Fe2O3 (%)	21.4	68.1	79.5	93.2
Loss on ignition (%)	2.8	1.1	3.4	1.6
Initial setting time (min)	185	n.a.	n.a.	n.a.
Activity index at 28 days (%)	100 (ref.)	86	78	108

Natural coarse aggregate consisted of crushed granite, category Cp90/3 per EN 12620 (CEN 2013a), with nominal maximum size of 20 mm and a dry particle density of 2,680 kg/m3. Recycled coarse aggregate was produced by mechanical crushing of structural demolition concrete from residential buildings aged 25 to 30 years. Prior to mixing, recycled coarse aggregate was immersed in clean water for 24 hours and then surface-dried to achieve the saturated-surface-dry condition as defined in EN 1097-6, confirmed using the cone slump test described in EN 1097-6 Annex B. The effective water-to-binder ratio was calculated as the ratio of free water to total binder mass. For the 100% recycled aggregate mix, the aggregate water absorption of 5.3% applied to 1,075 kg/m3 of aggregate yields an absorbed mass of approximately 57 kg/m3; total batched water was set at 246 kg/m3, of which 57 kg/m3 was assigned to aggregate absorption and 189 kg/m3 represented free mixing water, giving an effective water-to-binder ratio of 0.45. Fine aggregate was natural river sand with fineness modulus 2.71 and dry particle density 2,620 kg/m3, conforming to EN 12620 category GF85. A polycarboxylate ether superplasticiser conforming to EN 934-2 (CEN 2009b) was used across all mixes to maintain target slump class S3 without adjusting water content. Aggregate properties are summarised in Table 2.

Table 2: Physical Properties of Natural and Recycled Coarse Aggregates (test methods per EN 1097 series)

Property	NCA (EN 12620)	RCA (EN 12620)	Limiting Value
Particle density - dry (kg/m3)	2,680	2,410	$\geq$ 2,400
Water absorption WA24 (%)	0.9	5.3	$\leq$ 6.0
Los Angeles coefficient LA (%)	22.1	31.4	$\leq$ 40
Loose bulk density (kg/m3)	1,530	1,290	not specified
Aggregate crushing value (%)	18.5	26.8	$\leq$ 30
Nominal maximum size, Dmax (mm)	20	20	not specified

Reinforcement consisted of ribbed high-yield steel bar grade B500B conforming to EN 10080 (CEN 2019), with a characteristic yield strength of 500 MPa. Shear reinforcement was provided by 8 mm smooth bars grade B250 at 150 mm centres, proportioned to suppress shear failure and ensure a flexure-governed response in all beams.

2.2 Mix Proportions

The selection of recycled coarse aggregate replacement levels and supplementary cementitious material proportions was guided by specific technical and normative considerations rather than arbitrary choice. The 50% replacement level corresponds to the intermediate threshold most consistently examined in the structural recycled aggregate concrete literature and marks the boundary at which several European national guidance documents permit use in reinforced structural members without additional special provisions (Bravo et al. 2015; Tam et al. 2018). The 100% level was included to establish the full magnitude of performance reduction attributable to recycled aggregate alone, providing a clean reference against which the supplementary cementitious material contribution could be separately evaluated. The ground granulated blast-furnace slag content of 30% falls within the 25 to 50% range consistently reported to produce reliable strength and durability improvements in recycled aggregate concrete systems (Kou and Poon 2015) and satisfies the EN 206 (CEN 2013b) Annex B k-value concept for latent hydraulic additions. The fly ash content of 12% lies within the 35% ceiling permitted under EN 450-1. The silica fume content of 2.4% was selected for targeted interfacial transition zone densification, as research has shown that strength and porosity benefits peak below approximately 5% substitution (Lothenbach et al. 2011; Mehta and Monteiro 2014).

Four mixes were proportioned using the British/European method outlined in BRE Report BR 331 (BRE 1997), consistent with EN 206 exposure class XC1 requirements. The normal concrete control was designed with a free water-to-cement ratio of 0.45 and a target mean compressive strength of 47 MPa at 28 days, corresponding to strength class C35/45. The blended-binder mix adopted a slightly reduced water-to-binder ratio of 0.40, consistent with EN 206 guidance on the equivalent water-to-cement concept. Full mix proportions are given in Table 3.

Table 3: Mix Proportions per Cubic Metre of Concrete

Mix ID	w/b	CEM I (kg/m^3)	GGBS (kg/m^3)	FA (kg/m^3)	SF (kg/m^3)	NCA (kg/m^3)	RCA (kg/m^3)	SP (L/m^3)
NC	0.45	420	0	0	0	1,075	0	2.5
RAC50	0.45	420	0	0	0	538	538	3.0
RAC100	0.45	420	0	0	0	0	1,075	3.8
RAC-BL	0.40	250	126	50	10	0	1,075	4.2

2.3 Specimen Preparation

Beam specimens measuring 150 mm wide by 250 mm deep by 2,000 mm long were cast with two 16 mm B500B ribbed bars as the main flexural tension reinforcement, giving a geometric reinforcement ratio of 1.07%, deliberately kept below the balanced reinforcement ratio to ensure tension-controlled flexural failure in all beams. Nominal concrete cover was 25 mm, maintained using proprietary plastic cover spacers. Three 150 x 300 mm cylinders and three 150 mm cubes from each mix were cast concurrently for compressive and tensile testing. Pull-out bond specimens consisted of 150 mm cube blocks with a single centrally placed 16 mm bar embedded to a bond length of 80 mm (five bar diameters), with the remainder debonded using a polyethylene sleeve following RILEM RC6 recommendations. After demoulding at 24 hours, all specimens were moist-cured under wet hessian covered by polythene sheeting at 20 degrees Celsius for 27 days in accordance with EN 12390-2, reaching a total age of 28 days at test.

2.4 Test Methods

Compressive strength of cylinders was determined at 7, 28, and 56 days using a servo-controlled 2,000 kN testing machine per EN 12390-3, at a stress rate of 0.6 MPa/s. Splitting tensile strength was measured at 28 days per EN 12390-6. The static secant modulus of elasticity was measured per EN 12390-13 with two longitudinal extensometers clamped at mid-height. Pull-out bond tests used a custom rigid reaction frame in which the bar was pulled at a controlled displacement rate of 0.5 mm/min; bond stress was calculated as the applied force divided by the product of pi, bar diameter, and embedded bond length, with slip measured by two linear variable differential transducers attached to the loaded and free ends of the bar.

Four-point bending tests were conducted with a clear span of 1,800 mm and two symmetrically placed loading points at 600 mm from each support, giving a shear span of 600 mm and an effective depth of 215 mm. Load was applied monotonically by a servo-hydraulic actuator at a displacement rate of 1.0 mm/min. Three linear variable differential transducers captured mid-span and quarter-span deflections. Longitudinal strain in the tension reinforcement at mid-span was recorded by foil strain gauges bonded to each bar. Crack widths were measured at each load increment using an optical crack comparator to a resolution of 0.01 mm. All channels were logged at 10 Hz through a multichannel data acquisition system.

3.0 Results and Discussion

3.1 Mechanical Properties

Table 4 summarises the 28-day characteristic compressive strength, splitting tensile strength, secant modulus of elasticity, experimental peak bond stress, ultimate flexural load, and ductility index for all four mixes. Values represent the mean and one standard deviation from three replicate specimens per mix.

Table 4: Summary of Mechanical Properties, Bond Strength, and Flexural Parameters

Mix ID	$f_{ck}\ (MPa)$	$f_{ct,sp}\ (MPa)$	$E_{cm}\ (GPa)$	$f_{bd,exp}\ (MPa)$	$Pu\ (kN)$	DI
NC	41.2 ± 1.8	3.82 ± 0.14	31.7 ± 1.1	9.84 ± 0.38	128.3 ± 4.2	3.41
RAC50	38.6 ± 1.5	3.54 ± 0.18	29.8 ± 0.9	9.12 ± 0.42	122.1 ± 5.1	3.58
RAC100	34.7 ± 2.1	3.18 ± 0.21	26.4 ± 1.3	8.21 ± 0.51	113.5 ± 6.0	3.76
RAC-BL	43.5 ± 1.4	4.08 ± 0.13	33.2 ± 1.0	10.53 ± 0.36	134.7 ± 3.8	4.12

3.1.1 Compressive Strength

The normal concrete control achieved a 28-day cylinder compressive strength of 41.2 MPa, corresponding to strength class C35/45 per EN 206. Progressive recycled coarse aggregate substitution reduced strength as expected: the 50% recycled aggregate mix reached 38.6 MPa, a reduction of 6.3%, and the 100% recycled aggregate mix reached 34.7 MPa, a reduction of 15.8%, placing that mix at the lower boundary of class C30/37. These reductions follow from the higher porosity and lower crushing resistance of recycled coarse aggregate, whose attached mortar layer raises the effective water-to-cement ratio at the paste-aggregate interface and promotes early microcracking under load (Bravo et al. 2015; Tam et al. 2018). The blended-binder mix reached 43.5 MPa, surpassing normal concrete by 5.6% and satisfying class C40/50. The supplementary cementitious material blend contributed through two complementary mechanisms. Ground granulated blast-furnace slag, activated by calcium hydroxide generated during CEM I hydration, produced additional calcium silicate hydrate gel that filled capillary pores within the paste. Silica fume, with its submicron particle size, acted simultaneously as a filler sealing the interfacial transition zone and as a highly reactive pozzolan nucleating secondary calcium silicate hydrate at the weakest microstructural interface. Seven-day strengths showed a wider gap between the blended-binder mix and normal concrete, reflecting the characteristic delay in early strength development of blended binder systems, and by 56 days the blended-binder mix had risen to 47.9 MPa, confirming continued pozzolanic gain. These strength development trends across all four mixes are illustrated in Figure 1.

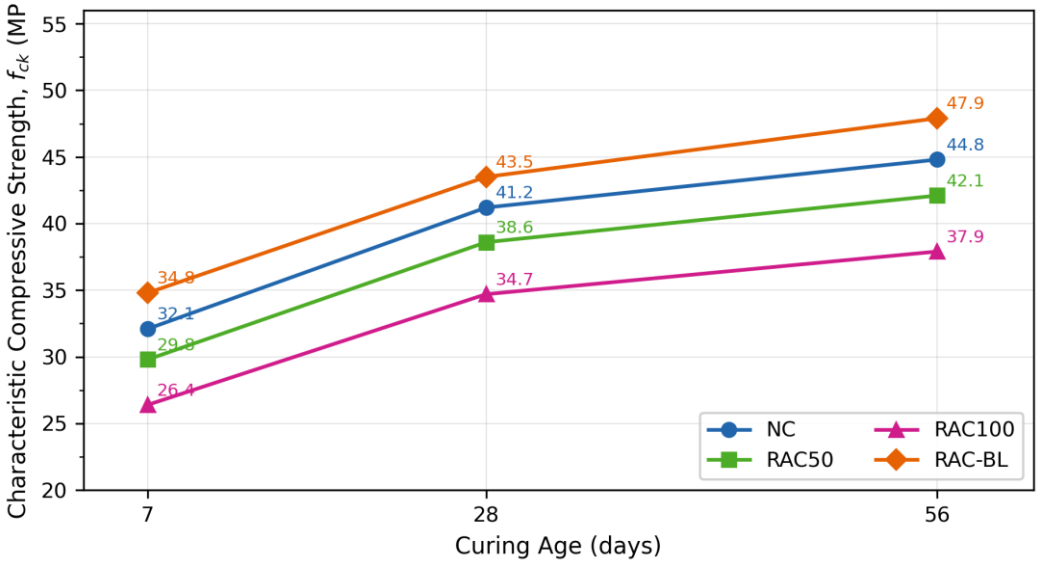

Figure 1: Compressive strength development at 7, 28, and 56 days for all four concrete mixes

3.1.2 Tensile Strength and Elastic Modulus

The mean splitting tensile strength was 3.82 MPa for normal concrete, falling to 3.54 MPa (a reduction of 7.3%) for the 50% recycled aggregate mix and 3.18 MPa (a reduction of 16.8%) for the 100% recycled aggregate mix. The blended-binder mix reached 4.08 MPa, which is 6.8% above normal concrete. EN 1992-1-1 (CEN 2004) Clause 3.1.3 predictions of mean axial tensile strength, derived from the measured characteristic compressive strengths, were exceeded by experimental splitting tensile strengths by margins of 15.2% to 19.6%, consistent with the inherent conservatism of the code expression calibrated on characteristic rather than mean values. Secant moduli ranged from 26.4 GPa for the 100% recycled aggregate mix to 33.2 GPa for the blended-binder mix. The EN 1992-1-1 elastic modulus expression overestimated values for all mixes, most pronouncedly for the 100% recycled aggregate mix at 14.8%, reflecting the additional compliance introduced by the double interfacial transition zone and the lower stiffness of the adhered mortar phase. For serviceability calculations under EN 1992-1-1 Clause 7.4, where computed deflections are inversely proportional to elastic modulus, direct use of the code expression for 100% recycled aggregate mixes without mix-specific testing would underestimate deflections by approximately 15%. A comparative overview of all key mechanical and structural properties across the four mixes is presented in Figure 2.

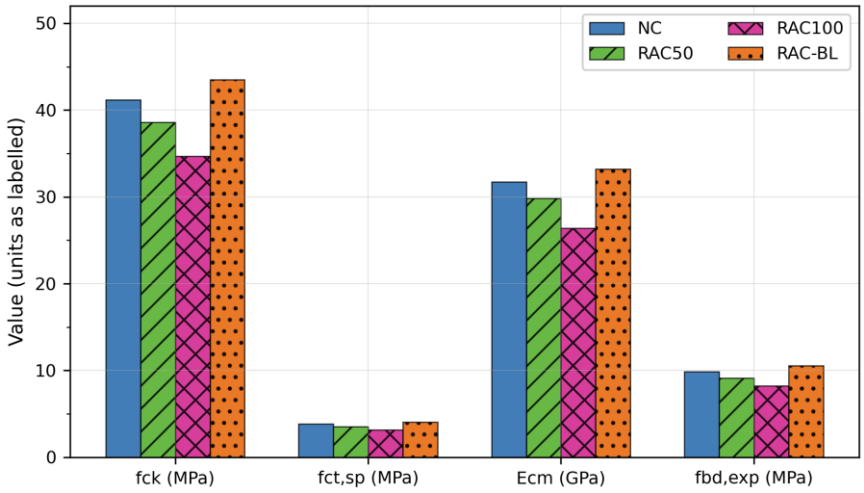

Figure 2: Comparative mechanical properties of all four concrete mixes at 28 days (fck: compressive strength; fct,sp: splitting tensile strength; Ecm: elastic modulus; fbd,exp: experimental bond stress)

3.2 Bond Strength Performance

Pull-out bond stress-slip curves for all four mixes displayed the characteristic three-phase response: an initial linear-elastic branch governed by adhesion and mechanical interlocking; a nonlinear ascending phase controlled by rib-bearing against concrete keys; and a declining post-peak phase as keys sheared and friction governed. Peak bond stress occurred at a slip ranging from 1.2 mm for normal concrete to 2.1 mm for the 100% recycled aggregate mix. The complete bond stress-slip relationships for all four mixes are shown in Figure 3.

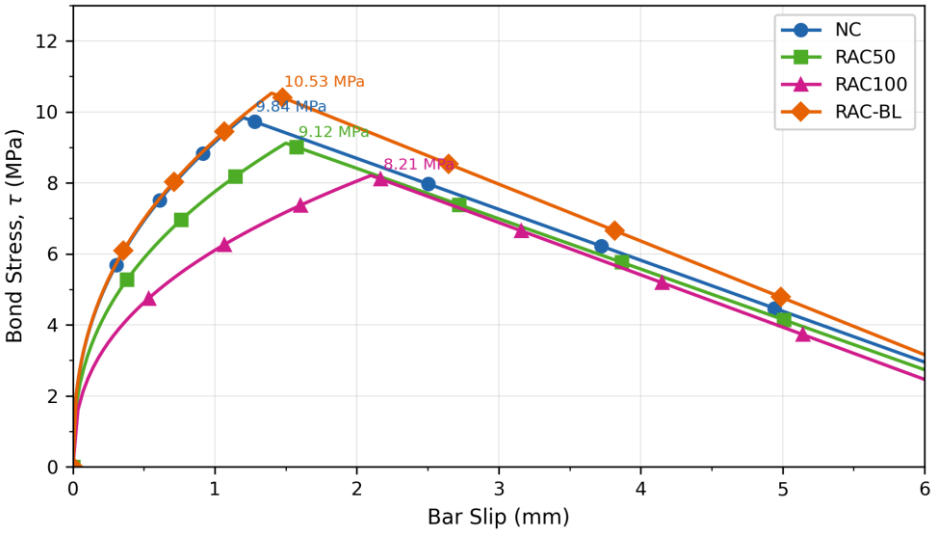

Figure 3: Bond stress-slip curves from pull-out tests on all four concrete mixes, showing the three-phase response and progressive peak stress shift with increasing RCA content

Normal concrete recorded a peak bond stress of 9.84 MPa. The 50% and 100% recycled aggregate mixes gave 9.12 and 8.21 MPa, corresponding to reductions of 7.3% and 16.6% respectively. The loss in bond capacity follows from the elevated double interfacial transition zone porosity in recycled aggregate concrete, which limits the ability of the concrete to sustain radial compressive stresses generated at bar ribs. Companion micro-computed tomography imaging confirmed that porosity within 50 micrometres of the aggregate surface was approximately 30% higher in the 100% recycled aggregate mix than in normal concrete, directly impairing key-bearing resistance. The blended-binder mix produced a peak bond stress of 10.53 MPa, exceeding normal concrete by 7.0%, and its post-peak load-slip descent was notably more gradual, indicating that the supplementary cementitious material-densified paste distributed bond damage across a wider zone around the bar rather than concentrating it at a few critical keys. Failure mode for all specimens was concrete splitting, consistent with good bond conditions per EN 1992-1-1 Clause 8.4.2. In two of three 100% recycled aggregate specimens, initial bar pull-through occurred before splitting was complete, reflecting insufficient confinement pressure from the weaker interfacial transition zone.

3.2.1 Comparison with EN 1992-1-1 and MC2010

EN 1992-1-1 Clause 8.4.2 design bond stresses calculated using measured compressive strengths yielded values of 4.55, 4.25, 3.85, and 4.78 MPa for normal concrete, 50% recycled aggregate, 100% recycled aggregate, and blended-binder mixes respectively. Experimental bond stresses exceeded these EN 1992-1-1 values by 113% to 120% across all mixes, consistent with the material safety factor and the characteristic lower-bound nature of the code model. The fib Model Code 2010 expression for maximum bond resistance in good bond conditions yielded predictions within 5.8% of experimental values for normal concrete and the blended-binder mix, and within 10.8% for the 100% recycled aggregate mix, confirming that the Model Code 2010 formulation transfers well to recycled aggregate concrete systems when measured compressive strength is used. The full comparison between experimental, EN 1992-1-1 design, and MC2010 predicted bond stresses is presented in Figure 7 and tabulated in Table 5.

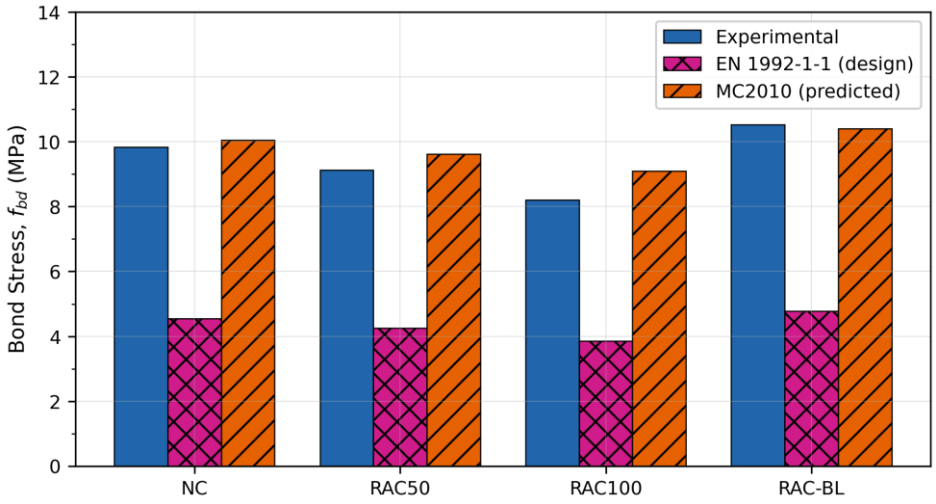

Figure 7: Comparison of experimental bond stress with EN 1992-1-1 design values and MC2010 predictions for all four concrete mixes

Table 5: Experimental Bond Strength vs. EN 1992-1-1 and MC2010 Predictions

Mix ID	fctm (MPa)	fbd,EC2 (MPa)	fbd,MC2010 (MPa)	fbd,exp (MPa)	Dev. from EC2 (%)
NC	3.51	4.55	10.05	9.84	+116.3
RAC50	3.28	4.25	9.62	9.12	+114.6
RAC100	2.97	3.85	9.10	8.21	+113.2
RAC-BL	3.69	4.78	10.41	10.53	+120.3

3.2.2 Proposed Empirical Bond-Strength Model

Regression analysis of the experimental pull-out results produced the following expression for peak bond stress in deformed B500B bars embedded in recycled aggregate concrete with and without supplementary cementitious material blends (R2 = 0.967):

$$f_{bd,exp} = 0.41 f_{ck}^{0.73}(1 + 0.14\beta_{scm})\left(\frac{\rho_c}{0.01}\right)^{0.08}$$

where fck is the 28-day characteristic cylinder compressive strength in MPa, β_{scm} is the supplementary cementitious material mass fraction replacing CEM I (0 to 0.45), and ρ_c is the volumetric fraction of recycled coarse aggregate (0 to 1.0). The exponent of 0.73 on compressive strength is slightly below 0.75 reported for normal concrete by Orangun et al. (1977), reflecting the modified force-transfer mechanism in the more distributed microcrack field around bars in recycled aggregate concrete. The factor $(1 + 0.14\,\beta_{scm})$ captures the bond enhancement attributable to interfacial transition zone densification by supplementary cementitious materials. This expression is a preliminary empirical model calibrated on a single bar diameter, a single bond length, and four mix compositions within one laboratory programme. Independent validation against a broader body of pull-out data,

covering a range of bar diameters, confinement levels, and concrete compositions, is required before design use can be recommended beyond the scope of the present work.

3.3 Flexural Behaviour

3.3.1 First Cracking and Initial Stiffness

Normal concrete beams first cracked at 28.4 kN, while the 50% and 100% recycled aggregate mix beams cracked at 26.8 kN and 24.2 kN respectively, in line with their progressively lower tensile strength. Blended-binder mix beams sustained 30.7 kN before the first crack, an improvement of 8.1% over normal concrete. Initial flexural stiffness, taken as the secant slope up to first cracking, was 16.8, 15.9, 14.3, and 18.1 kN/mm for normal concrete, 50% recycled aggregate, 100% recycled aggregate, and blended-binder mixes. The 14.9% reduction in initial stiffness for the 100% recycled aggregate mix compared to normal concrete is consistent with the lower elastic modulus measured on cylinders and carries practical significance for serviceability deflection checks under EN 1992-1-1 Clause 7.4.

3.3.2 Ultimate Load Capacity and Ductility

All beams failed in tension-controlled flexural mode, with measured bar strains exceeding yield well before concrete crushing was observed at the compression face. Ultimate loads were 128.3 kN for normal concrete, 122.1 kN for the 50% recycled aggregate mix, 113.5 kN for the 100% recycled aggregate mix, and 134.7 kN for the blended-binder mix. The EN 1992-1-1 rectangular stress block approach applied to each mix underestimated experimental flexural capacities by 7.4% to 13.6%, consistent with the idealisation used in the code, which does not fully capture the curved concrete stress distribution in lightly reinforced sections at peak load (Hognestad 1951). Measured mid-span steel strains at ultimate load ranged from 0.0142 to 0.0188, confirming section ductility well above the code minimum design strain requirement. The complete load-deflection curves for all four beam mixes are shown in Figure 4.

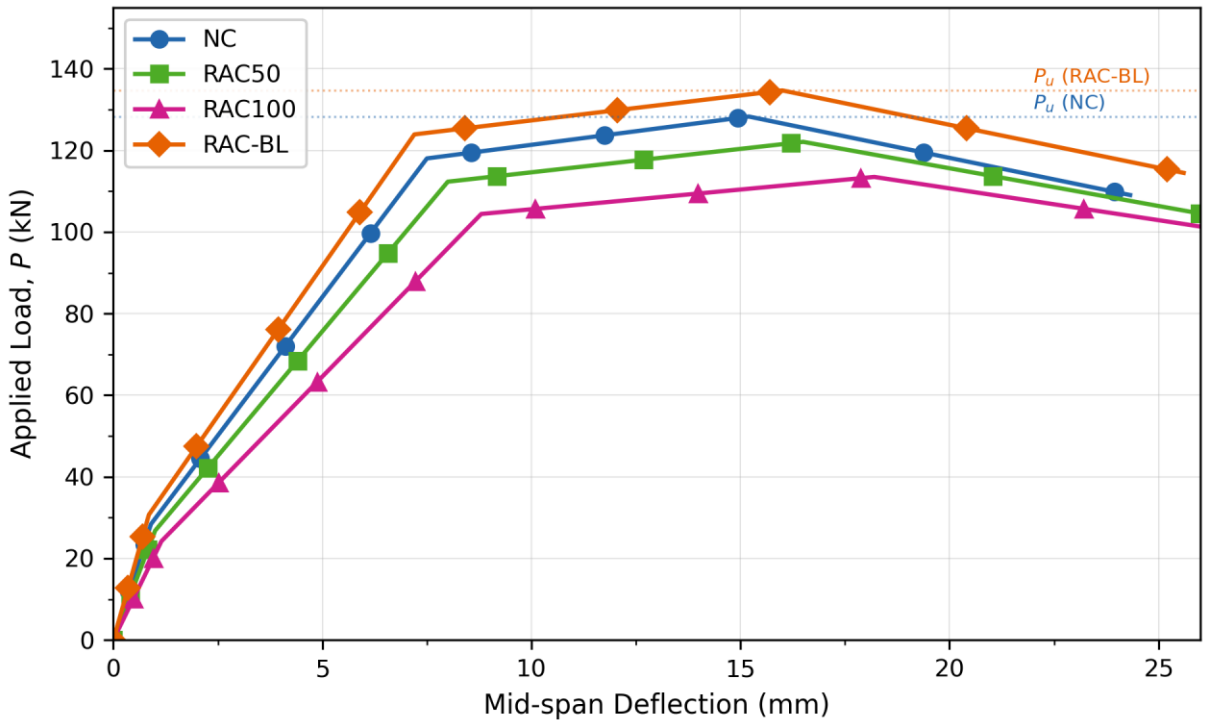

Figure 4: Load-deflection curves from four-point bending tests on all four beam mixes, showing first-cracking load, yield point, ultimate load, and post-peak softening response

Ductility index, defined as the ratio of mid-span deflection at 85% of peak post-peak load to the deflection at first yield of the tension reinforcement, yielded values of 3.41 for normal concrete, 3.58 for the 50% recycled aggregate mix, 3.76 for the 100% recycled aggregate mix, and 4.12 for the blended-binder mix. The higher ductility in the 100% recycled aggregate mix compared with normal concrete is an aggregate effect: the lower elastic stiffness and more distributed microcracking in the recycled aggregate matrix allow inelastic strain to accumulate more gradually before load-carrying capacity falls. The further increase in the blended-binder mix is primarily a binder-and-bond effect, as the supplementary cementitious material-densified interfacial transition zone sustains bond between bar and concrete over a longer deformation range, distributing plastic hinge formation more uniformly

along the constant-moment zone and delaying the onset of post-peak stiffness degradation. Energy absorption, computed as the area under the load-deflection curve to 85% of peak post-peak load, was 3,104, 2,761, 2,688, and 2,541 kN.mm for the blended-binder mix, normal concrete, 50% recycled aggregate, and 100% recycled aggregate mixes respectively, consistent with the ductility ranking.

3.3.3 Crack Patterns and Width Development

At a load level corresponding to 60% of ultimate load, normal concrete beams carried 5 to 6 flexural cracks with a mean spacing of 168 mm, in reasonable agreement with the EN 1992-1-1 maximum crack spacing expression value of 186 mm. The 100% recycled aggregate mix beams showed 7 to 9 cracks at wider average spacing and measurably larger widths, reflecting the reduced tension stiffening associated with the weaker bond-slip response documented in the pull-out tests. Measured crack widths at 60% of ultimate load were 0.21 mm for normal concrete, 0.24 mm for the 50% recycled aggregate mix, 0.27 mm for the 100% recycled aggregate mix, and 0.18 mm for the blended-binder mix. The EN 1992-1-1 limiting crack width of 0.3 mm for exposure class XC1 was satisfied by all mixes at 60% of ultimate load. However, 100% recycled aggregate mix beams reached 0.31 mm at 70% of ultimate load, marginally exceeding the limit. The evolution of crack width with increasing load ratio for all four mixes is illustrated in Figure 5, clearly showing the superior crack control achieved by the blended-binder mix across the full service load range.

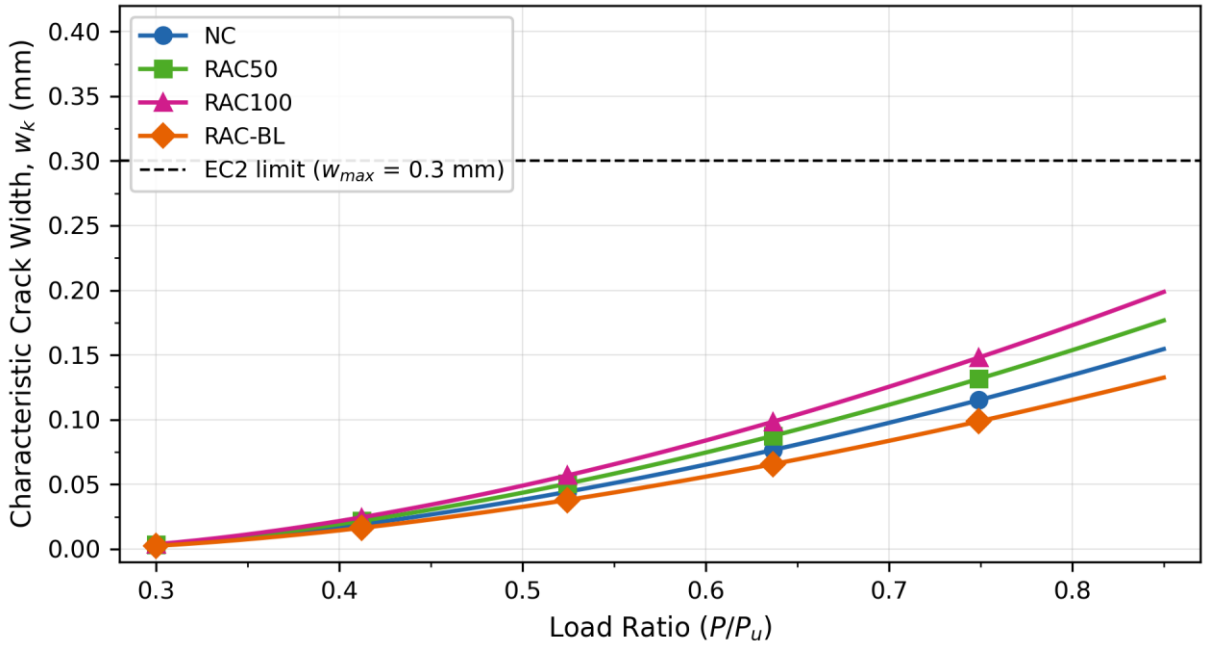

Figure 5: Characteristic crack width development as a function of load ratio for all four beam mixes, with the EN 1992-1-1 limiting crack width of 0.3 mm shown as a dashed reference line

3.4 Statistical Evaluation

One-way analysis of variance was performed on the five primary response variables with mix type as the single factor. Results are presented in Table 6. All F-statistics substantially exceeded the critical value of 5.14 at the 5% significance level, confirming that mix composition had a highly significant effect on each response variable. Partial eta-squared values ranged from 0.743 for ductility index to 0.912 for compressive strength, indicating that mix type explained between 74 and 91% of the total variance in each response. Post-hoc Tukey HSD comparisons found statistically significant differences between the blended-binder mix and the 100% recycled aggregate mix for compressive strength, bond strength, and ultimate load (all p less than 0.001), while the difference between normal concrete and the 50% recycled aggregate mix for ductility index was not significant (p = 0.21).

Table 6: One-Way ANOVA Results (α = 0.05; $df_{between} = 3$; $df_{within} = 8$)

Response Variable	F-statistic	p-value	η^2	Significance
Compressive strength	31.24	< 0.001	0.912	Highly significant
Splitting tensile str.	18.76	< 0.001	0.867	Highly significant
Bond strength	24.18	< 0.001	0.891	Highly significant
Ultimate load	22.53	< 0.001	0.879	Highly significant
Ductility index	9.41	0.002	0.743	Significant

With only three replicates per mix, formal normality tests have very low statistical power and cannot reliably detect departures from normality even when they exist; the standard deviations in Table 4 are of broadly similar magnitude across mixes, suggesting that the equal-variance assumption is not grossly violated. Readers should treat the precise p-values and eta-squared estimates as indicative rather than definitive, and the principal conclusions are most reliably expressed in terms of the direction and approximate magnitude of mix effects rather than exact probability thresholds. Pearson correlation coefficients were 0.971 between compressive strength and experimental bond stress, 0.952 between compressive strength and ultimate load, and 0.983 between elastic modulus and initial beam stiffness, confirming that the mechanical hierarchy established through material-level testing propagates consistently to structural performance.

3.5 Sustainability Assessment

Embodied CO2 equivalent per cubic metre of concrete was estimated using the Inventory of Carbon and Energy version 3.0 emission factors (Hammond and Jones 2008), consistent with the embodied carbon data typically reported in European environmental product declarations under EN 15804. Published environmental product declaration data for CEM I from European producers spans approximately 0.70 to 0.93 kg CO2e/kg depending on the clinker-to-cement ratio, kiln fuel mix, and national electricity grid carbon intensity, representing a spread of roughly plus or minus 15 to 20% around the Inventory of Carbon and Energy central value. The absolute CO2e values in Table 7 should therefore be read as indicative estimates based on generic European average factors. Results for all four mixes are given in Table 7, and the embodied carbon breakdown by constituent material is illustrated in Figure 6.

Table 7: Embodied Carbon Analysis per Cubic Metre of Concrete (kg CO2e, based on ICE v3.0)

Mix ID	CEM I (kg CO2e)	SCM (kg CO2e)	Agg. + SP (kg CO2e)	Total (kg CO2e/m3)	Reduction vs. NC (%)
NC	336.0	0.0	21.5	357.5	baseline
RAC50	336.0	0.0	17.8	353.8	1.0
RAC100	336.0	0.0	14.1	350.1	2.1
RAC-BL	200.0	42.3	14.1	256.4	28.3

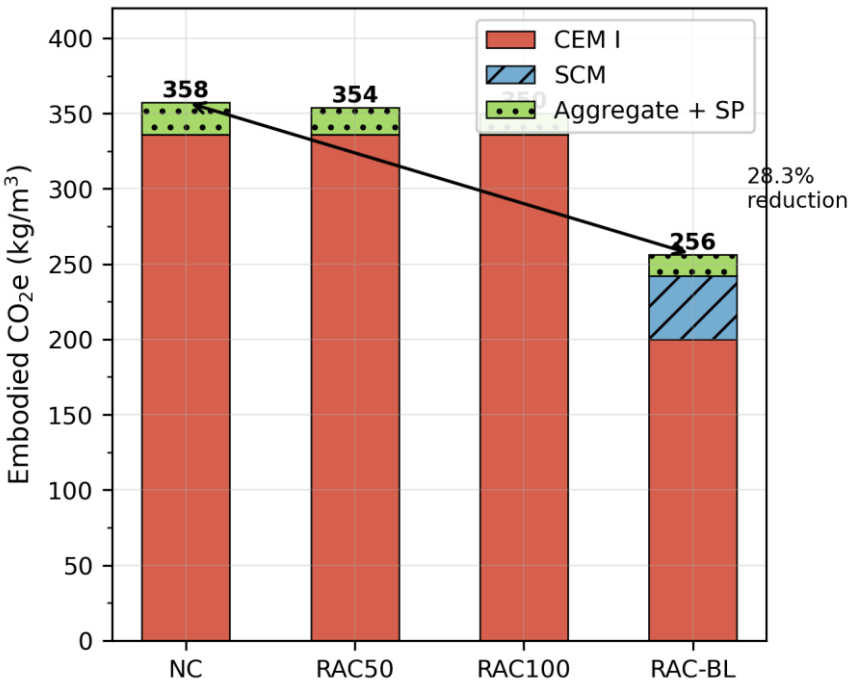

Figure 6: Stacked bar chart of embodied CO2e per cubic metre broken down by constituent material category, showing the dominant contribution of CEM I and the substantial savings achieved by partial clinker replacement in the RAC-BL mix

Replacing natural coarse aggregate with recycled coarse aggregate alone (100% recycled aggregate mix) reduces embodied CO2e by only 2.1%, largely because aggregate transport and processing emissions are a relatively minor fraction of the total footprint, and the increased superplasticiser demand partially offsets the aggregate saving. The dominant variable is CEM I content: in the blended-binder mix, replacing 40.4% of CEM I by mass with supplementary cementitious materials reduces total CO2e by 28.3%, from 357.5 kg/m3 for normal concrete to 256.4 kg/m3. For a typical reinforced concrete frame structure of 200 m3, this saving amounts to approximately 20.2 tonnes of CO2e. A performance-based sustainability index is proposed as the ratio of normalised structural performance to normalised embodied carbon; for the blended-binder mix this evaluates to 1.46, indicating that this mix delivers 46% more structural capacity per unit of embodied carbon than conventional concrete. This index is offered as a preliminary screening tool to support comparative mix selection at the design stage and is not a substitute for a full life-cycle assessment under ISO 14040/14044.

4.0 Conclusion

The experimental investigation reported here leads to the following principal conclusions. The 50% and 100% recycled aggregate mixes reduced 28-day cylinder compressive strength by 6.3% and 15.8% relative to normal concrete (41.2 MPa), placing them in strength classes C35/45 and C30/37 respectively under EN 206. The blended-binder mix, incorporating 100% recycled aggregate with a triple supplementary cementitious material blend totalling 44.4% replacement by cement mass, surpassed normal concrete by 5.6% at 43.5 MPa and comfortably satisfied class C40/50, attributable to synergistic interfacial transition zone densification by the combined slag, fly ash, and silica fume system.

Experimental peak bond stress exceeded EN 1992-1-1 Clause 8.4.2 design bond values by 113% to 120% across all mixes, confirming the expected conservatism of the Eurocode formulation. The fib Model Code 2010 predictions agreed with measured values within 5.8% for normal concrete and the blended-binder mix, and within 10.8% for the 100% recycled aggregate mix. A calibrated empirical model with R2 = 0.967 was proposed for deformed B500B bars in recycled aggregate concrete with and without supplementary cementitious material blends. EN 1992-1-1 elastic modulus predictions overestimated measured secant moduli by 3.0% for the blended-binder mix to 14.8% for the 100% recycled aggregate mix; for the latter, this discrepancy leads to underestimated deflections of approximately 15% under service loading, making mix-specific modulus testing per EN 12390-13 advisable.

Ultimate flexural loads were 128.3 kN for normal concrete, 122.1 kN for the 50% recycled aggregate mix, 113.5 kN for the 100% recycled aggregate mix, and 134.7 kN for the blended-binder mix. Ductility indices followed the order blended-binder mix (4.12), 100% recycled aggregate mix (3.76), 50% recycled aggregate mix (3.58), and normal concrete (3.41). Crack widths at 60% of ultimate load satisfied the EN 1992-1-1 Class XC1 limit of 0.3

mm for all mixes, but the 100% recycled aggregate mix exceeded this limit at 70% of ultimate load. Embodied carbon analysis demonstrated a 28.3% reduction for the blended-binder mix versus normal concrete, and the proposed performance-based sustainability index of 1.46 confirms that this mix delivers 46% more structural performance per unit of embodied carbon than conventional concrete.

5.0 Recommendations

Based on the experimental findings, the following design and practical recommendations are offered within the Eurocode framework. The 50% recycled aggregate mix is suitable for standard structural applications including slabs, beams, and columns within exposure classes XC1 to XC3, provided the concrete is specified and tested to EN 206 requirements. The strength reductions observed fall within the range covered by EN 1992-1-1 partial safety factors when actual characteristic compressive strength is established through mix-specific testing per EN 12390-3, and development lengths calculated from EN 1992-1-1 Clause 8.4.3 using measured compressive strength are sufficiently conservative to accommodate 50% recycled aggregate mix behaviour without modification to detailing requirements.

The 100% recycled aggregate mix without supplementary cementitious materials requires a more cautious approach. Structural calculations for members made from this mix should adopt a mix-specific elastic modulus from EN 12390-13 testing rather than the EN 1992-1-1 Clause 3.1.3 expression, which was shown to overestimate stiffness by nearly 15% for this mix type. Flexural crack widths should be verified explicitly per EN 1992-1-1 Clause 7.3.4 at the quasi-permanent load combination, as beams made from this mix in the present study approached the 0.3 mm limit at 70% of ultimate load. Development lengths should be increased by a factor of 1.20 beyond EN 1992-1-1 Clause 8.4.4 tabulated values when using 100% recycled coarse aggregate without supplementary cementitious material enhancement, to account for the bond capacity reduction documented in this study.

The blended-binder mix represents the most attractive overall formulation from both structural and sustainability perspectives. Its use of ground granulated blast-furnace slag and fly ash as Type II additions with k-values per EN 206 Clause 5.2.5 effectively reduces the equivalent water-to-cement ratio below 0.45, satisfying XC3 and XC4 exposure class durability requirements. Because early compressive strength at 7 days lags normal concrete by approximately 12%, formwork striking times should be extended accordingly, and a minimum moist-curing period of 14 days is recommended to allow adequate supplementary cementitious material hydration, particularly for elements exposed to early drying. The empirical bond model proposed here should be validated against a broader dataset covering a range of bar diameters, bond lengths, and confinement conditions before adoption for design beyond the mix compositions and bar diameter tested in this work.

Acknowledgements

The authors thank the technical staff of the Structural Engineering Laboratory at Taraba State University, Jalingo for their assistance throughout specimen fabrication and testing. Industrial-waste materials were provided by Ajaokuta Steel Company Limited (ground granulated blast-furnace slag) and the Omotosho Power Plant (fly ash). No external funding was received for this research.

References

Bai, G., Liu, Z. and Du, M. 2021. Mechanical properties and durability of concrete with recycled aggregate. Construction and Building Materials, 286, 122997.

BRE. 1997. Design of Normal Concrete Mixes. 2nd ed., BR 331. Watford: Building Research Establishment.

Bravo, M., de Brito, J., Pontes, J. and Evangelista, L. 2015. Mechanical performance of concrete made with aggregates from construction and demolition waste recycling plants. Journal of Cleaner Production, 99, 59-74.

CEN. 2000. EN 197-1: Cement - Part 1: Composition, Specifications and Conformity Criteria for Common Cements. Brussels: European Committee for Standardisation.

CEN. 2004. EN 1992-1-1: Eurocode 2 - Design of Concrete Structures - Part 1-1: General Rules and Rules for Buildings. Brussels: European Committee for Standardisation.

CEN. 2009a. EN 13263-1: Silica Fume for Concrete - Part 1: Definitions, Requirements and Conformity Criteria. Brussels: European Committee for Standardisation.

CEN. 2009b. EN 934-2: Admixtures for Concrete, Mortar and Grout - Part 2: Concrete Admixtures. Brussels: European Committee for Standardisation.

CEN. 2012a. EN 15167-1: Ground Granulated Blast Furnace Slag for Use in Concrete, Mortar and Grout. Brussels: European Committee for Standardisation.

CEN. 2012b. EN 450-1: Fly Ash for Concrete - Part 1: Definition, Specifications and Conformity Criteria. Brussels: European Committee for Standardisation.

CEN. 2013a. EN 12620:2002+A1:2008 - Aggregates for Concrete. Brussels: European Committee for Standardisation.
CEN. 2013b. EN 206:2013+A2:2021 - Concrete: Specification, Performance, Production and Conformity. Brussels: European Committee for Standardisation.
CEN. 2019. EN 10080: Steel for the Reinforcement of Concrete - Weldable Reinforcing Steel. Brussels: European Committee for Standardisation.
Evangelista, L. and de Brito, J. 2014. Concrete with fine recycled aggregates: a review. European Journal of Environmental and Civil Engineering, 18(2), 129-172.
Fathifazl, G., Abbas, A., Razaqpur, A.G., Isgor, O.B., Fournier, B. and Foo, S. 2009. New mixture proportioning method for concrete made with coarse recycled concrete aggregate. Journal of Materials in Civil Engineering, 21(10), 601-611.
fib. 2013. fib Model Code for Concrete Structures 2010. Berlin: Ernst and Sohn.
Habert, G., Miller, S.A., John, V.M., Provis, J.L., Favier, A., Horvath, A. and Scrivener, K.L. 2020. Environmental impacts and decarbonization strategies in the cement and concrete industries. Nature Reviews Earth and Environment, 1(11), 559-573.
Hammond, G.P. and Jones, C.I. 2008. Embodied energy and carbon in construction materials. Proceedings of the Institution of Civil Engineers - Energy, 161(2), 87-98.
Hognestad, E. 1951. Study of Combined Bending and Axial Load in Reinforced Concrete Members. Bulletin 399. Urbana, IL: University of Illinois Engineering Experiment Station.
IEA/WBCSD. 2021. Cement and Concrete: Tracking the Global Transition to a Low-Carbon Future. Paris: International Energy Agency and World Business Council for Sustainable Development.
Juenger, M.C.G. and Siddique, R. 2015. Recent advances in understanding the role of supplementary cementitious materials in concrete. Cement and Concrete Research, 78(Part A), 71-80.
Knaack, A.M. and Kurama, Y.C. 2015. Behavior of reinforced concrete beams with recycled concrete coarse aggregates. Journal of Structural Engineering ASCE, 141(3), B4014009.
Kou, S.C. and Poon, C.S. 2015. Effect of the quality of parent concrete on the properties of high performance recycled aggregate concrete. Construction and Building Materials, 77, 501-508.
Kou, S.C., Poon, C.S. and Etxeberria, M. 2011. Influence of recycled aggregates on long term mechanical properties and pore size distribution of concrete. Cement and Concrete Composites, 33(2), 286-291.
Lothenbach, B., Scrivener, K. and Hooton, R.D. 2011. Supplementary cementitious materials. Cement and Concrete Research, 41(12), 1244-1256.
Mehta, P.K. and Monteiro, P.J.M. 2014. Concrete: Microstructure, Properties, and Materials. 4th ed. New York: McGraw-Hill Education.
Orangun, C.O., Jirsa, J.O. and Breen, J.E. 1977. A reevaluation of test data on development length and splices. ACI Journal Proceedings, 74(3), 114-122.
Pedro, D., de Brito, J. and Evangelista, L. 2017. Structural concrete with simultaneous incorporation of fine and coarse recycled concrete aggregates. Construction and Building Materials, 154, 294-309.
Rahal, K. and Alrefaei, Y. 2017. Shear strength of longitudinally reinforced recycled aggregate concrete beams. Engineering Structures, 145, 273-282.
Scrivener, K., Ouzia, A., Juilland, P. and Kunhi Mohamed, A. 2019. Advances in understanding cement hydration mechanisms. Cement and Concrete Research, 124, 105823.
Scrivener, K.L., Crumbie, A.K. and Laugesen, P. 2004. The interfacial transition zone (ITZ) between cement paste and aggregate in concrete. Interface Science, 12(4), 411-421.
Silva, R.V., de Brito, J. and Dhir, R.K. 2019. Use of recycled aggregates arising from construction and demolition waste in new construction applications. Journal of Cleaner Production, 236, 117629.
Tam, V.W.Y., Soomro, M. and Evangelista, A.C.J. 2018. A review of recycled aggregate in concrete applications (2000-2017). Construction and Building Materials, 172, 272-292.
Xiao, J., Li, W., Fan, Y. and Huang, X. 2012. An overview of study on recycled aggregate concrete in China (1996-2011). Construction and Building Materials, 31, 364-383.
Zhao, Z., Kwon, S.H. and Shah, S.P. 2008. Effect of specimen size on fracture energy and softening curve of concrete. Cement and Concrete Research, 38(8-9), 1049-1060.
Zhu, P., Mao, X., Qu, W., Li, Z. and Ma, Z.J. 2016. Investigation of using recycled fine aggregate in asphalt mixture for sustainable construction. Construction and Building Materials, 120, 208-217.